where ρ = 1,225 kg/m^3 air density; C_x = 0,3 drag coefficient or longitudinal aerodynamic force coefficient; A_f = 2 m^2 transversal section of vehicle including wheels and parts under floor; v_r is vehicle speed in m/s. Constant data used in (1) are for typical sedan car. Then aerodynamic torque at wheels T_{aer} is evaluated with equation (2):

(2) $$T_{aer} = \frac{1}{2}\rho C_x A_f v_r^2 r_d$$

where r_d = 0,28 m radius of rolling defined as radius of rigid wheel that translate and rotate at same speed of pneumatic wheel. And in the end, aerodynamic power at wheels P_{aer} is evaluated through equation (3) and plotted in Figure 62:

(3) $$P_{aer} = \frac{1}{2}\rho C_x A_f v_r^3$$

Fig. 62: aerodynamic power versus vehicle speed

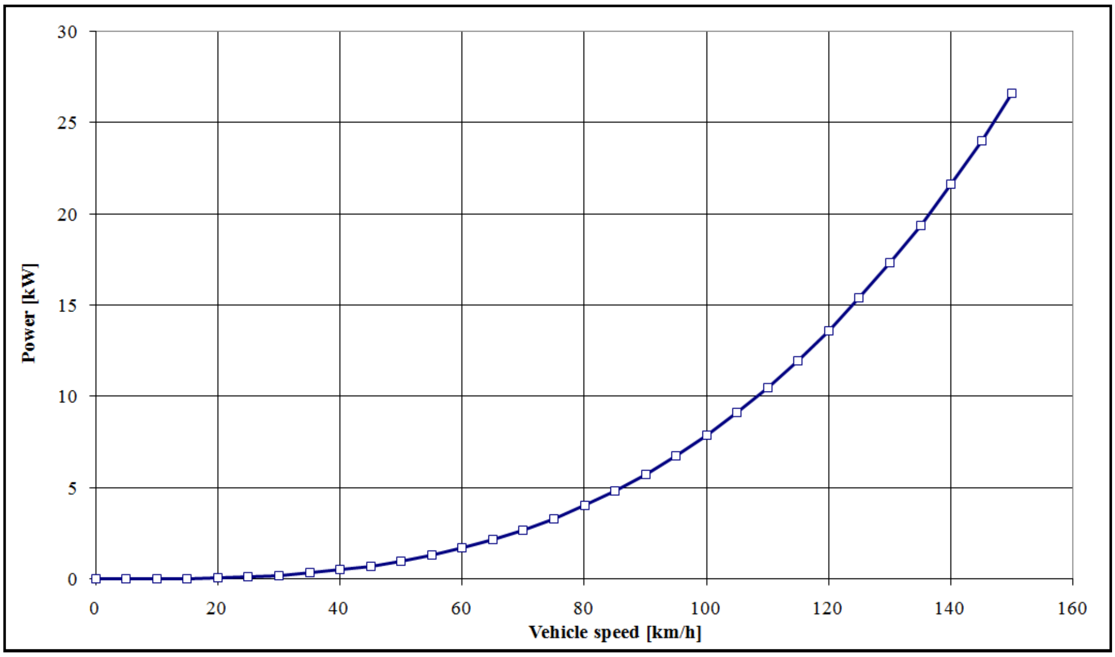

Figure 62 shows aerodynamic power and highlights growth trend at power of three of vehicle speed. Moreover, under 50 % of vehicle speed range, aerodynamic power contribution is less than 20 % of the maximum power.
About slope resistance, it could evaluate in the same way of aerodynamic resistance, through force, torque and then power. Slope force at wheels F_{sl} is calculated with equation (4):

(4) $$F_{sl} = m\ g\ \sin\alpha$$

where m = 1400 kg is full load vehicle mass in test condition or in according with SAE guide lines, vehicle mass in Standard C that means vehicle mass with all liquids with maximum load for vehicle, maximum number of passengers plus load per each passengers; g = 9,81 m/s^2, α is related to percentage slope i in according to (5) and (6):

(5) $$i = 100\ \tan\alpha$$

(6) $$\alpha = \tan^{-1}\left(\frac{i}{100}\right)$$

In this example, road slope is set at 4 % that means every 100 meters along road steps 4 meters. Slope torque at wheels T_{sl} is evaluated through equation (7):

(7) $$T_{sl} = m\ g\ \sin\alpha\, r_d$$

And in the end, slope power at wheels P_{sl} is calculated by equation (8) and plotted in Figure 63:

(8) $$P_{sl} = m\ g\ \sin\alpha\ v_r$$

Fig. 63: slope power versus vehicle speed

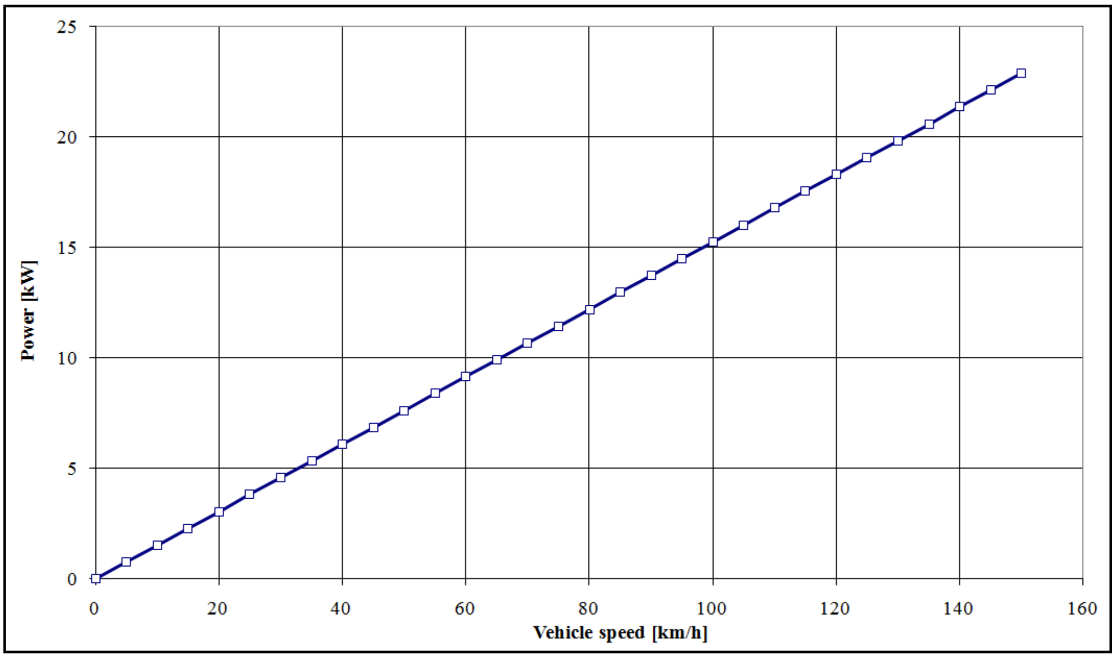

Figure 63 shows slope power versus vehicle speed and highlights linear relation between power and speed at constant slope.

Flat rolling resistance is mainly related to rolling coefficient *f* as well as slope rolling resistance. *f* increases with vehicle speed increase, in the beginning very slowly and then faster and faster, see Figure 64.

Fig. 64: rolling coefficient *f* trend versus vehicle speed. a) measure on radial and conventional tire; b) experimental curve – radial tire 5,20-14 inflated at 190kPa with 340 kN load – compared with equation (11)

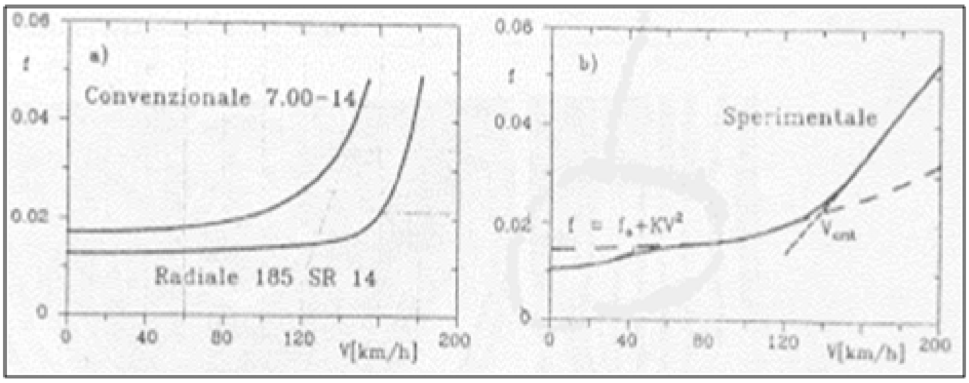

Relationship *f (V)* could be approximate with polynomial expression in form of (9):

(9) $$f = \sum_{i=0}^{n} f_i v_r^i$$

In general, one considers two terms of equation (9) are enough to approximate in proper way experimental trend of *f (V)*, at last up to vehicle speed which rolling coefficient *f* starts to rocket as highlighted in Figure 64. It could use follow equation:

(10) $$f = f_0 + f_2 v_r$$

or

(11) $$f = f_0 + f_2 v_r^2$$

Equation (11) is usually preferred to (10) but in industrial application in case of unavailable data, one could use equation (12):

(12) $$f = k_r$$

Equations (11) and (12) are plotted in Figure 65.

Fig. 65: constant and speed related rolling coefficient comparison

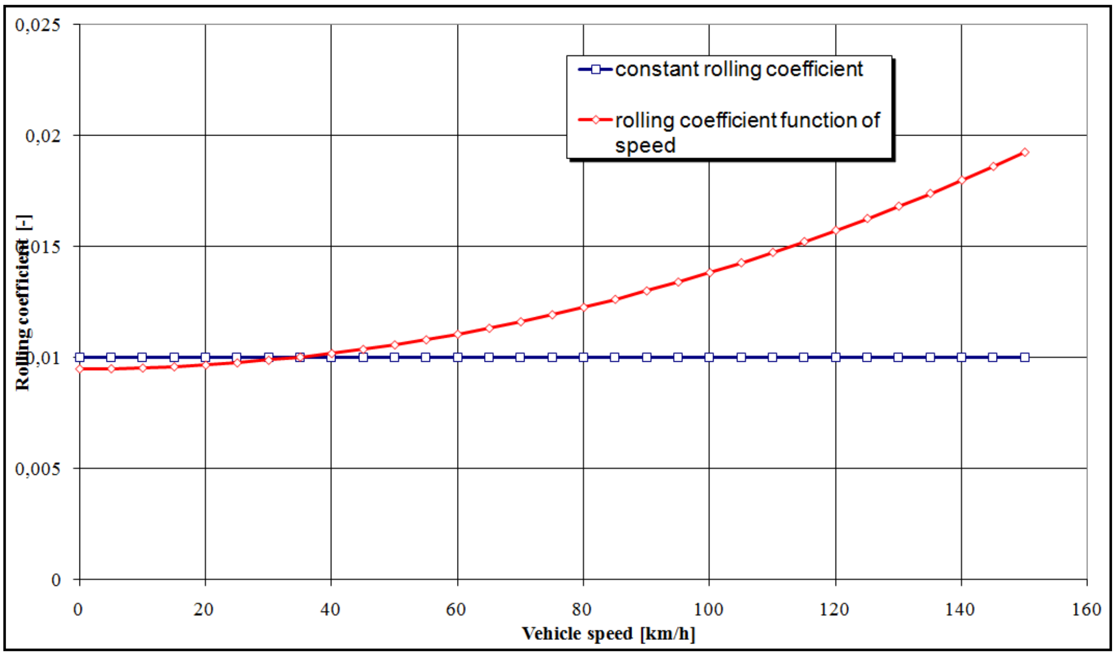

Figure 65 highlights rolling coefficient trend evaluated through (11) is strongly related with velocity at power of two. f_0 and f_2 values are evaluated experimentally tire per tire; for example in case of Figure 64b and in that test conditions, values are respectively 0,013 and 6,5 $\cdot$ 10^{-6} s^2/m^2. Velocity where *f (V)* has knee, is tire critical velocity. Existence of tire critical velocity could easily explain through vibration phenomena happen at high speed. Flat rolling force at wheels F_{rot}^{fl} according with equations (12) and (11) is evaluated respectively in equations (13) and (14):

(13) $$F_{rot}^{fl} = m\, g\, k_r$$

(14) $$F_{rot}^{fl} = m\, g\, (f_0 + f_2 v_r^2)$$

where k_r = 10^{-2} [-], $f_0 = 9{,}5 \cdot 10^{-3}$ $[-]$, $f_2 = 5{,}6 \cdot 10^{-6}$ $\left[\frac{s^2}{m^2}\right]$. In this case *m* is vehicle mass in Standard E that mean vehicle mass with all liquids plus two passengers and load for each passenger. Flat rolling torque at wheels T_{rot}^{fl} is calculated trough equations (15) and (16):

(15) $$T_{rot}^{fl} = m\ g\ k_r\ r_d$$

(16) $$T_{rot}^{fl} = m\ g\ (f_0 + f_2 v_r^2)\ r_d$$

And in the end, flat rolling power at wheels P_{rot}^{fl} is computed by equations (17) and (18) and plotted in Figure 66:

(17) $$P_{rot}^{fl} = m\ g\ k_r\ v_r$$

(18) $$P_{rot}^{fl} = m\ g\ (f_0 + f_2 v_r^2)\ v_r$$

Fig. 66: flat rolling power resistance comparison with constant and speed related rolling coefficient

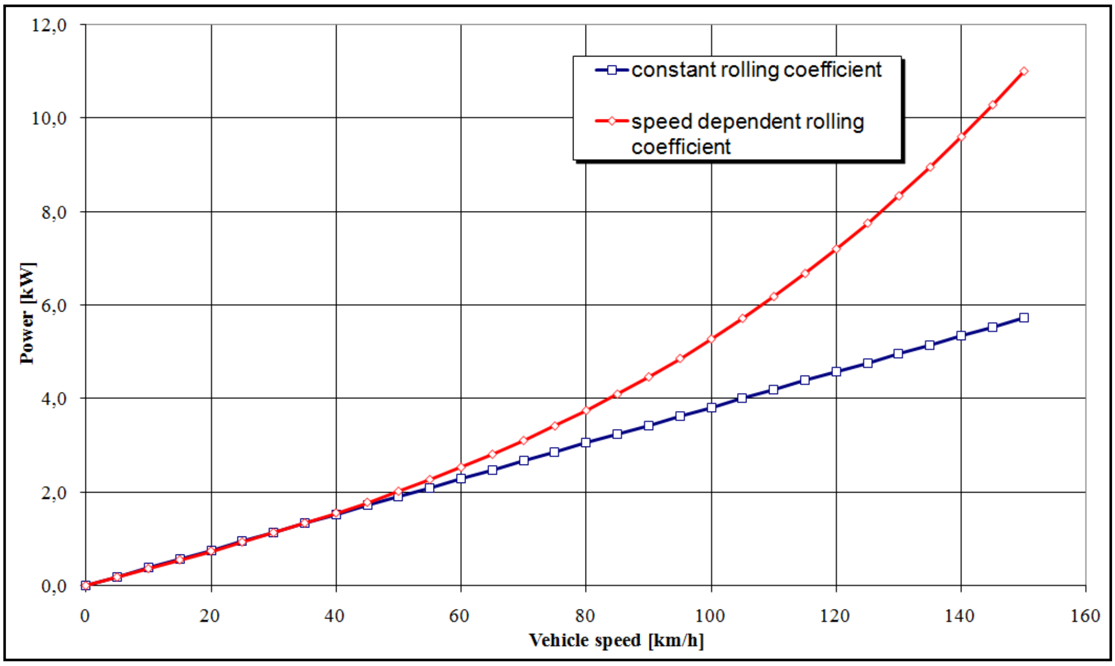

Under 40 km/h, constant rolling coefficient follow better experimental data respect to speed related one. But, as shown in Figure 66, flat rolling power resistance evaluated in both way gives pretty same result and for this reason equation (12) is preferred one. Otherwise, equation (12) is usable up to 70 km/h, or in others words up to error between equations (17) and (18) is acceptable.

In case of slope road, slope rolling resistance is evaluate as usual through force, torque and power. Slope rolling force at wheels F_{rot}^{sl} is evaluated by equations (19) and (20):

(19) $$F_{rot}^{sl} = m\, g\, k_r\, \cos\alpha$$

(20) $$F_{rot}^{sl} = m\, g\, (f_0 + f_2 v_r^2)\, \cos\alpha$$

α is computed in the same way as before and in particular with equations (5) and (6).

While slope rolling torque at wheels T_{rot}^{sl} is calculated through equations (21) and (22):

(21) $$T_{rot}^{sl} = m\, g\, k_r\, \cos\alpha\ r_d$$

(22) $$T_{rot}^{sl} = m\, g\, (f_0 + f_2 v_r^2)\, \cos\alpha\ r_d$$

And finally, slope rolling power resistance P_{rot}^{sl} is evaluated through equations (23) and (24) and plotted in Figure 67:

(24) $$P_{rot}^{sl} = m\, g\, k_r\, \cos\alpha\ v_r$$

(25) $$P_{rot}^{sl} = m\, g\, (f_0 + f_2 v_r^2)\, \cos\alpha\ v_r$$

Fig. 67: slope rolling power resistance comparison with constant and speed related rolling coefficient

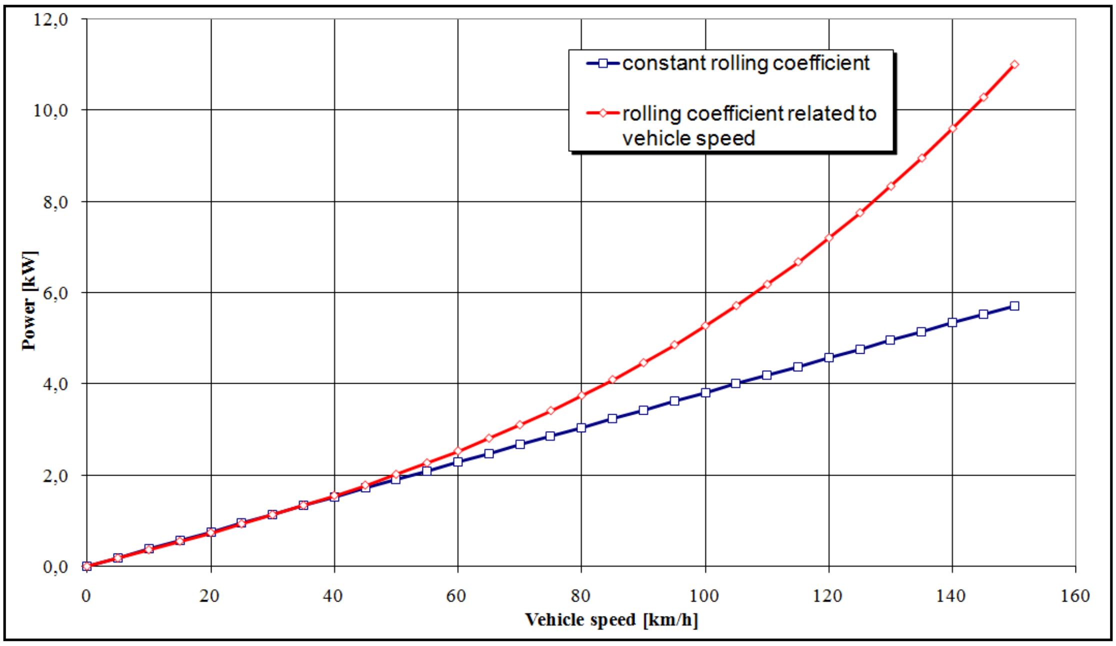

Total power resistance P_{tot} is sum of different contributions and in particular depends on flat, (26) or slope (27) road:

(26) $$P_{tot} = P_{aer} + P_{rot}^{fl}$$

(27) $$P_{tot} = P_{aer} + P_{rot}^{sl} + P_{sl}$$

Figure 68 shows total power resistance for slope road at 4 %.

Fig. 68: total power resistance using constant rolling resistance

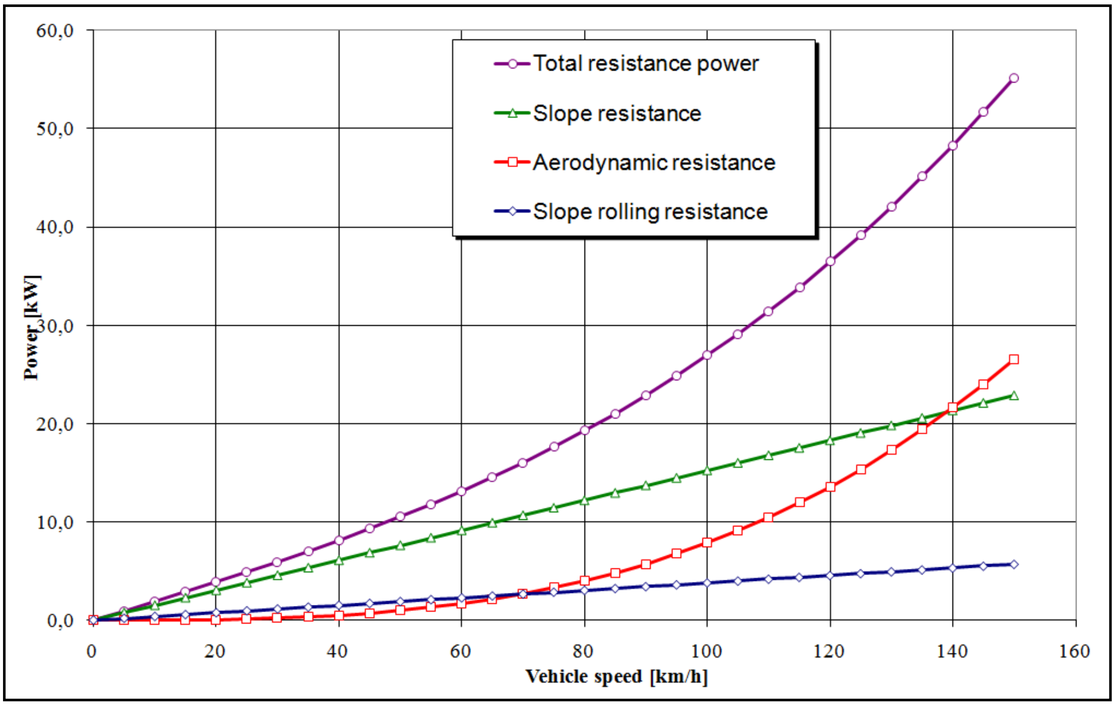

Usually for flat road, it is very important determine characteristic speed of vehicle defined as vehicle velocity where aerodynamic resistance power equals rolling resistance power. Now, if power curve of IC engine is plotted in Figure 68, it intercepts total resistance power curve at certain point that show maximum vehicle speed. Distance between total resistance curve and IC engine power curve is exuberant power and vehicle uses it to accelerate. At this point, one could verify acceleration that exuberant power can get to vehicle. In this way, target power curve of IC engine could verify and modified to achieve target SAE performance index of vehicle as defined through equation (28):

(28) $P.I. = acc.0 - 100 + acc.60 - 100\ in\ IV + acc.80 - 120\ in\ V + 1000\ at\ V_{max}$

where: *acc. 0-100* is time in seconds to accelerate vehicle from 0 to 100 km/h; *acc. 60-100 in IV* is time in seconds to accelerate vehicle from 60 to 100 km/h in IV gear; *acc. 80-120 in V* is time in seconds to accelerate vehicle from 80 to 120 km/h in V gear; *1000*

at V_{max} is time in seconds to travel 1000 m at maximum vehicle speed. In particular vehicle performance index is used to link Customer Car Profile with Quality Profile in term of vehicle brilliancy.
First step to understand if IC engine has enough exuberant power or, in the other side, one could evaluate vehicle acceleration with present exuberant power, is calculate mass apparent sliding of vehicle m_{as} in test conditions.

(29) $$m_{as} = m + \frac{J_{ICE}\,\tau_{ICE-whe}^2}{r_d^2} + \frac{J_{tra}\,\tau_{tra-whe}^2}{r_d^2} + \frac{J_{whe}}{r_d^2}$$

where m is vehicle mass in test conditions in Standard C for slope cases and Standard E for flat cases measured in [kg]; J_{ICE} is IC engine inertia in [kg m^2]; $\tau_{ICE-whe}$ transmission ratio between IC engine and wheels defined through equation (30); J_{tra} is transmission inertia in [kg m^2]; $\tau_{tra-whe}$ is transmission ratio between transmission and wheels in [-] defined by equation (31); J_{whe} is wheels inertia [kg m^2].

(30) $$\tau_{ICE-whe} = \frac{\omega_{ICE}}{\omega_{whe}}$$

(31) $$\tau_{tra-whe} = \frac{\omega_{tra}}{\omega_{whe}}$$

where ω_{ICE} is angular engine speed; ω_{tra} is angular speed of transmission; ω_{whe} is angular speed of wheels. Now, with apparent mass sliding m_{as} could evaluate dynamic force at wheels F_{dyn} through equation (32):

(32) $$F_{dyn} = m_{as}\, a$$

where a is vehicle acceleration in [m/s^2]. Then, dynamic torque at wheels T_{dyn} is evaluated through equation (33):

(33) $$T_{dyn} = m_{as}\, a\, r_d$$

And in the end, dynamic power at wheels is evaluated with equation (34):

(34) $$P_{dyn} = m_{as}\, a\, v_r$$

Usually, this kind of analysis are carried on with commercial software as GT-Drive [87] that allow to study vehicle performance and vehicle – propulsion system matching. Basically, GT-Drive works in three different mode: static, kinematic and dynamic. In static mode, the solver creates a wide group of main performance index – power and torque, vehicle acceleration, … - on the whole engine speed range for every transmission rate; the engine load that the solver uses to calculate these index is defined by '*static mode load factor*'. In kinematic mode it is possible calculate the performance requirements and the emissions for cycles as NEDC; the vehicle speed is imposed and the solver calculates the engine performances. In dynamic mode is possible evaluate the transient performances – e.g. 0 – 100 km/h test –; the engine load is specified and the solver calculates the vehicle answer.

I-V Reference

1. Brambilla E., "Si fa presto a dire hybrid", QuattroRuote, Vol. 1, 2011, pp. 110 – 117

2. Ford, www.ford.com

3. General Motors, www.generalmotors.com

4. U.S. Department of Energy – Energy Efficiency & Renewable Energy and U.S. Environmental Protection Agency – Office of Transportation & Air Quality, www.fueleconomy.gov

5. Hybrid cars – Auto alternatives for 21st century, www.hybridcars.com

6. Toyota, www.toyota.com

7. Hybrid cars, www.hybridcenter.com

8. Automotive Manual PDF – The resources for Automotive, www.autosmanual.com

9. Polk, www.polk.com

10. Crouse W. H., Anglin D. L., "Automotive Engines – Construction, Operation and Maintenance", 8th Eds, Glencoe, 1994

11. Garro A., "Progettazione Strutturale del Motore", Levrotto & Bella, Torino, 1992

12. Vignocchi D., "Elementi di Progettazione del Motore", Athena, 2002

13. Alu Matter, www.aluminium.matter.co.uk

14. MatWeb - Metal Property Data, www.matweb.com

15. Takami T., Fujine M., Kato S., Nagai H., Tsujino A., Masuda Y.-H., Yamamoto M., "MMC All Aluminum Cylinder Block for High Power SI Engines", SAE Technical Paper 2000-01-1231, SP-1495, CI and SI Power Cylinder Systems

16. Delprete C., "Engine Design", Master Program in Automotive Engineering - Powertrain, Politecnico di Torino, 2006

17. Perrone A., Bonollo F., Wagner V., "Fonderia: Stato dell'Arte", Alluminio Magazine, 4 (Agosto 1998), 32 – 41

18. Cantor B., Grant P., Johnston C., "Automotive Engineering – Lightweight, Functional and Novel Materials", Taylor & Francis, 2008

19. Zovko Brodarac Z., Mrvar P., Medved J., Fajfar P., "Local Squeezing Casting Influence on the Compactness of AlSi9Mg Alloy Casting", Metalurgija 46 (2007) 1, 29 – 35

20. Reichelt W., Voss-Spilker P., Urlau U., Keutgen K., Willems E., "Method on and apparatus for spraycasting", US Patent 5060713

21. WKW Automotive, www.wkw.de

22. Clarke M., "Quale Tecnologia per i Cilindri in Alluminio", AutoTecnica, 1999, Vol. 2, 26 – 32

23. Austrian Institute of Technology, www.lkr.at

24. Darton Sleeves, "Honda Installation Manual – Modular Integrated Deck", 2004

25. Akalin O., Newaz G. M., Durga V., Rao N., "Friction Characteristics of Plasma Spray Coated Cylinder Bores", SAE Technical Paper 1999-01-1220

26. Kamo L., Saad P., Saad D., Bryzik W., Mekari M. H., "Diesel Engine Cylinder Bore Coating for Extreme Operating Conditions", SAE Technical Paper 2007-01-1439, SP-2073, CI and SI Power Cylinder Systems, 2007

27. Cupitò G., Trabucco D., "An Integrated Methodology for the Stress Evaluation of Aluminum Casting Components", ATA - Ingegneria dell'Autoveicolo, Vol.60, 11/12 2007, 22 – 28

28. Hamm T., Rebbert M., Ecker H.-J., Grafen M., “Cylinder Head Design for High Peak Firing Pressures”, SAE Technical Paper 2008-01-1196

29. Zhang B., Albertinazzi M., Scotti F., Sarietto G., Garro M., “Tensile Properties and Residual Stresses of a Diesel Cylinder Head in GAS9C1 Alloy”, SAE Technical Paper 2005-01-1692, SP-1948, Lightweight Castings and Aluminum Alloys for Advanced Automotive Applications

30. Garro M., Zhang B., “Factors Affecting Residual Stresses of Cylinder Heads and Engine Blocks in Aluminum Alloys”, ATA Ingegneria dell’Autoveicolo, Vol. 60, pp. 32 – 39, 2007

31. Su X., Lasecki J., Jan J., Engler-Pinto Jr. C., Allison J., “Residual Stress Analysis of Air-Quenched Engine Aluminum Cylinder Heads”, SAE Technical Paper 2008-01-1420, SP-2192, Experiments in Automotive Engineering, 2008

32. Uraki Y., Kondo M., Yashiro H., “Development of a Technique for using Oil Viscosity to Reduce Noise Radiated from the Oil Pan”, SAE Technical Paper 1999-01-1759, P-342, Proceedings of the 1999 Noise and Vibration Conference

33. Wolff K., Lahey H.-P., Nussmann C., Nehl J., Wimmel R., Siebald H., Fehren H., Redaelli M., Naake A., “Active Noise Concellation at Powertrain Oil Pan”, SAE Technical Paper 2007-01-2422

34. Koike S., Washizu K., Tanaka S., Baba T., Kikawa K., “Development of Lightweight Oil Pans Made of a Heat-Resistant Mgnesium Alloy for Hybrid Engines”, SAE Technical Paper 2000-01-1117

35. Vert P., Niu X., Stickler A., Zaton W., Aghion E., “Comparative Evaluation of Automotice Oil Pans Fabricated by Creep Resistant Magnesium Alloy and Aluminum Alloy”, SAE Technical Paper 2004-01-0658, SP-1845, Magnesium for Automotive Components

36. Duran T. E., Sever C. A., “Puma I5 Diesel Engine Oil Pan Assembly NVH Optimization with Optistruct and AVL-Excite”, SAE Technical Paper 2008-01-2721

37. Kolekar A., Anderson M., Nash D., Hegde R., Puckett M., “New Generation Oil Pan Modules”, SAE Technical Paper 2009-01-0346

38. Suzuki S., Ozasa T., Noda T., Konomi T., “Analysis of Con-Rod Big-End Bearing Lubrication on the Basis of Oil Supply Rate”, SAE Technical Paper 982439, SP-1389, Passenger Car and Diesel Engine Lubricants

39. Xu H., Wang D. C., Poynton W. A., “Effects of Oil Groove Locations on the Performance of the Big End Bearing of a Medium Speed Diesel Engine”, SAE Technical Paper 1999-01-1316

40. Sato K., Makino K., Machida K., “A Study of Oil Film Pressure Distribution on Connecting Rods Big Ends”, SAE Technical Paper 2002-01-0296

41. Kosaka N., Yamaguti T., Sakai T., Lindberg C., “Evaluation of Press & Sinter Connecting Rods with Warm Compaction Process”., SAE Technical Paper 2000-01-0402, SP-1535, Powdered Metal Applications

42. Skoglund P., Bengtsson S., Bergkvist A., Sherborne J., Gregory M., “Performance of High Density P/M Connecting Rods”, SAE Technical Paper 2000-01-0403, SP-1535, Powdered Metal Applications

43. Geiman T., Christopherson D., Marra M., Williams R., “Machinability and Performance of Precision Powder Forged Connecting Rods”, SAE Technical Paper 2001-01-0351, SP-1610, Powdered Metal Performance Applications

44. Ilia E., Chernenkoff R. A., "Impact of Decarburization on the Fatigue Life of Powder Metal Forged Connecting Rods", SAE Technical Paper 2001-01-0403, SP-1610, Powdered Metal Performance Applications

45. Takada K., Kogure R., Sato M., Takada M., "Development of High Fatigue Strength for Powder-Forged Connecting Rods", SAE Technical Paper 2008-01-0849

46. Ilia E., O'Neill M., Tutton K., "Higher Fatigue Strength Materials for Powder Metal Forged Connecting Rods", SAE Technical Paper 2002-01-0611, SP-1681, Powder Metal Applications and Components

47. Ilia E., Tutton K., O'Neill M., Lanni G., Letourneau S., "New Improvements in Materials Used to Manfucature Powder Forged Connecting Rods", SAE Technical Paper 2007-01-1556

48. Suzuki H., Sawayama T., Ilia E., Tutton K., "New Material with Improved Machinability and Strength for Powder Forged Connecting Rods", SAE Technical Paper 2006-01-0603, SP-2039, Powder Metallurgy, 2006

49. Afzal A., Fatemi A., "A Comparative Study of Fatigue Behaviour and Life Predictions of Forged Steel and PM Connecting Rods", SAE Technical Paper 2004-01-1529, SP-1837, Innovations in Steel and Bar Products and Processing, and Modelling and Testing of Steel Structures

50. Hoffmann G., Geiman T., Marra M., Williams R., "Fracture Splitting of Powder Forged Connecting Rods", SAE Technical Paper 2002-01-0609, SP-1681, Powder Metal Applications and Components

51. Lee C. K., Ko Y. S., Kim S. H., Park H. S., Lim J. D., “Development of High Strength, Fracture Split Steel Connecting Rods”, SAE Technical Paper 2007-01-1002, SP-2103, “Steel Innovations, Fatigue Research, Sheet/Hydro/Gas Forming Technology & Advanced High Strength Steel Development”

52. Kato S., Kano T., Hobo M., Yamada Y., Miyazawa T., Okada Y., “Development of Microalloyed Steel for Fracture Split Connecting Rod”, SAE Technical Paper 2007-01-1004, SP-2103, “Steel Innovations, Fatigue Research, Sheet/Hydro/Gas Forming Technology & Advanced High Strength Steel Development”

53. Kubota T., Iwasaki S., Isobe T., Koike T., “Development of Fracture Splitting Method for Case Hardened Connecting Rods”, SAE Technical Paper 2004-32-0064

54. Park H., Ko Y. S., Jung S. C., Song B. T., Jun Y. H., Lee B. C., Lim J. D., “Development of Fracture Split Steel Connecting Rods”, SAE Technical Paper 2003-01-1309, SP-1764, Innovations in Steel Sheet & Bar Products

55. Londhe A., Yadav V., Sen A., “Finite Element Analysis of Connecting Rod and Correlation with Test”, SAE Technical Paper 2009-01-0816

56. Chacon H., “Structural and Fatigue Numerical Analysis for Connecting Rods Development”, SAE Technical Paper 2006-01-2515

57. Lee K. W., Chang H., Oh J. H., Kim Y. N., “Geometric Effects on Stiffness in Big End Structure of Connecting Rod”, SAE Technical Paper 2006-01-0390, SP-2032, Reliability and Robust Design in Automotive Engineering

58. Merritt D., Zhu G., “The Prediction of Connecting Rod Fretting and Fretting Initiated Fatigue Fracture”, SAE Technical Paper 2004-01-3015, SP-1898, “Diesel Particulate Systems, Engines and Components, and Performance Additives”

59. Suzuki M., Iijima S., Maehara H., Moriyoshi Y., "Effect of the Ratio between Connecting – Rod Length and Crank Radius on Thermal Efficiency", SAE Technical Paper 2006-32-0098

60. Durante E., "L'Equilibramento del Motore – I Parte", AutoTecnica, Vol. 2, 2004, pp. 122 – 128

61. Durante E., "L'Equilibramento del Motore – II Parte", AutoTecnica, Vol. 3, 2004, pp.127 – 133

62. Nuti M., "L'Equilibratura dei Motori a C. I. Alternativi – Parte I", AutoTecnica, Vol. 4, 2001, pp. 126 – 132

63. Nuti M., "L'Equilibratura dei Motori a C. I. Alternativi – Parte II", AutoTecnica, Vol. 7, 2001, pp. 138 – 143

64. Clarke M., "Gli Equilibratori Dinamici", AutoTecnica, Vol. 10, 1998, pp. 40 – 46

65. Suh K.-H., Lee Y.-K., Yoon H.-S., "A Study on the Balancing of the Three-Cylinder Engine with Balance Shaft", SAE Paper 2000-01-0601, SP-1515, Powertrain Systems NVH

66. Liu C. Q., Orzechowski J., "Theoretical and Practical Aspects of Balancing a V-8 Engine Crankshaft", SAE Paper 2005-01-2454

67. McLanahan C., Srinivasan S., Shulenberger A., "Compact Multi-Cylinder Z-Crank Axial Engine", SAE Technical Paper 2005-01-0651, SP-1978, "CI Engine Performance for Use with Alternative Fuels, and New Diesel Engines and Components"

68. Montazersadgh F. H., Fatemi A., “Optimization of a Forged Steel Crankshaft Subject to Dynamic Loading”, SAE Technical Paper 2008-01-0432, SP-2204, “Innovations in Steel and Applications of Advanced High Strength Steels for Automotive Structures”

69. Zuhdi N., Aziz F. N. A., Carden P., Bell D., “4 Versus 8 Counterweights for an I4 Gasoline Engine Crankshaft – Analytical Comparison”, SAE Technical Paper 2008-01-0088, SP-2180, Advanced Concepts

70. Londhe A., Yadav V. H., “Design and Optimization of Crankshaft Torsional Vibration Damper for a 4-Cylinder 4-Stroke Engine”, SAE Technical Paper 2008-01-1213, SP-2184, “Load Simulation and Analysis in Automotive Engineering”

71. Jiang Y., Festag G., Poe S., “Crankshaft Axial Vibration Analysis and Design Sensitivity Study”, SAE Technical Paper 2007-01-2298

72. Ko Y. S., Park J. W., Bham H. O., Park H., Lim J. D., “Fatigue Strength and Residual Stress Analysis of Deep Rolled Crankshafts”, SAE Technical Paper 2005-01-0988, SP-1951, “Innovations in Steel Sheet and Bar Products and Processing”

73. Choi K. S., Pan J., Ho S., “Effects of Roller Geometry on Contact Pressure and Residual Stress in Crankshaft Fillet Rolling”, SAE Technical Paper 2005-01-1908, SP-1957, Experiments in Automotive Engineering – Optical Techniques

74. Feng M., Li M., Gao L., “Duplex Surface Treatment of Pearlitic Ductile Iron for Diesel Crankshaft”, SAE Technical Paper 2005-01-1693, SP-1948, “Lightweight Castings and Aluminum Alloys for Advanced Automotive Applications”

75. Williams J., Fatemi A., “Fatigue Performance of Forged Steel and Ductile Cast Iron Crankshafts”, SAE Technical Paper 2007-01-1001, SP-2103, “Steel Innovations, Fatigue Research, Sheet/Hydro/Gas Forming Technology & Advanced High Strength Steel Development”

76. Spiteri P. V., Lee Y.-L., Segar R., “An Exploration of Failure Modes in Rolled, Ductile, Cast-Iron Crankshafts using a Resonant Bending Testing Rig”, SAE Technical Paper 2005-01-1906, SP-1957, “Experiments in Automotive Engineering – Optical Techniques”

77. Druschitz A. P., Fitzgerald D. C., Hoegfeldt I., “Lightweight Crankshafts”, SAE Paper 2006-01-0016, SP-2004, “New SI Engine and Component Design”

78. Asai T., Takitani Y., Sano N., Matsumoto H., “Strength Enhancement of Nitrocarburized Crankshaft Material”, SAE Paper 2008-01-0431, SP-2204, “Innovations in Steel and Applications of Advanced High Strength Steels for Automotive Structures”

79. AA VV, “Progetto di un Pistone Efficiente”, AutoTecnica, Vol. _, 2003, pp.134 – 136

80. Mansouri S. H., Wong V. W., “Effects of Piston Design Parameters on Piston Secondary Motion and Skirt-Liner Friction”, SAE Technical Paper 2004-01-2911, SP-1894, “Oils, Rheology, Tribology, and Driveline Fluids”

81. Tsujiuchi N., Koizumi T., Hamada K., Okamura M., Tsukijima H., “Optimization of Profile for Reduction of Piston Slap Exitation”, SAE Technical Paper 2004-32-0022

82. Bruni L., Casellato R., Matteoda P., Ongetta R., “The ‘X’ Piston – 5 Years Later”, _ 905189, _